[CANCER RESEARCH 62, 4263–4272, August 1, 2002]

Cilengitide Targeting of $\alpha_v\beta_3$ Integrin Receptor Synergizes with Radioimmunotherapy to Increase Efficacy and Apoptosis in Breast Cancer Xenografts[1]

Patricia A. Burke, Sally J. DeNardo,[2] Laird A. Miers, Kathleen R. Lamborn, Siegfried Matzku, and Gerald L. DeNardo

University of California at Davis, Sacramento Medical Center, Radiodiagnosis and Therapy/Internal Medicine, Sacramento, California 95816 [P. A. B., S. J. D., L. A. M., G. L. D.]; University of California at San Francisco, Department of Neurological Surgery, San Francisco, California 94143 [K. R. L.]; and Merck KGaA, Department of Preclinical Oncology, 64271 Darmstadt, Germany [S. M.]

ABSTRACT

Although metastatic breast cancer is responsive to radioimmunotherapy (RIT), a systemic targeted radiation modality, complete and permanent remissions are not typical with single-modality treatment. Antiangiogenic agents, which target normal, proliferating endothelial cells, have the potential to provide relatively nontoxic continuous inhibition of tumor growth by blocking new blood vessel growth and may synergize with RIT to increase efficacy. This study was designed to determine whether, and how, the cyclic Arg-Gly-Asp peptide Cilengitide (EMD 121974), which targets the $\alpha_v\beta_3$ integrin receptor expressed on neovasculature, could increase systemic RIT efficacy of therapy in a human breast cancer tumor model having mutant *p53* and expressing bcl-2. HBT 3477 breast cancer tumor response in nude mice was compared between groups of untreated mice ($n = 24$), Cilengitide-treated mice ($n = 18$), RIT (200–260 μCi ^{90}Y-labeled 1,4,7,10-tetraazacyclododecane-*N*,*N*′,*N*″,*N*‴-tetraacetic acid (DOTA)-peptide ChL6; n = 46), and combined modality RIT (CMRIT) using RIT and six doses of Cilengitide (250 μg/dose; n = 41). Tumor size, survival, body weight, and blood counts were monitored for efficacy and toxicity of therapy. To clarify the mechanism of synergistic effect, tumors were evaluated at selected time points through 6 days for apoptosis, proliferation, and microvessel density. Cilengitide alone did not alter tumor growth when compared with untreated mice, but CMRIT with Cilengitide increased efficacy of treatment, with the cure rate for mice that received 260 μCi RIT increasing from 15 to 53% ($P = 0.011$). Lower-dose RIT (200 μCi) combined with Cilengitide resulted in less increase in cures (36 compared with 25% for RIT alone; $P = 0.514$). Combined analysis for high- and low-dose groups demonstrated increased efficacy of CMRIT ($P = 0.020$). Analysis of tumors from CMRIT mice indicated significantly increased apoptosis of tumor and endothelial cells 5 days after RIT compared with tumors from mice given RIT alone. Proliferation was decreased in CMRIT tumors compared with RIT tumors at 6 days (ANOVA, $P < 0.05$). Microvessel density in tumors from RIT and CMRIT mice was not different. No increased toxicity attributable to Cilengitide was observed based upon pooled blood sample and no statistical increase in mortality. In conclusion, CMRIT, combining Cilengitide and RIT, significantly increased the efficacy of therapy and increased apoptosis compared with single-modality therapy with either agent, in an aggressive, well-studied breast cancer model. The enhanced therapeutic synergy is of particular note, having been achieved without additional toxicity.

INTRODUCTION

Novel and synergistic therapeutic combinations are required for the treatment of metastatic breast cancer, which is currently incurable with standard multimodality therapy (1). High incidence of *p53* mutations and bcl-2 protein overexpression in breast cancer increase resistance to chemotherapy and radiotherapy (2–9). Systemic, tumor-targeted RIT[3] has the potential to target tissue specifically and to deliver cancer-specific cytotoxic antibodies to widespread metastatic foci (10). However, studies in a human breast cancer xenograft model demonstrate that RIT, as a single agent, typically does not cure the tumors (1, 11). Tumor penetration of radiolabeled antibodies may be nonuniform and may not be sufficient in all regions of the tumor to provide cure (12, 13). The combination of RIT with other therapeutic modalities is currently being used (14), but the additional chemotherapy or external radiotherapy increases the risk of bone marrow toxicity (10, 11), the major dose-limiting factor in RIT (12).

Antiangiogenic agents may provide an alternative to increase efficacy of RIT without increasing toxicity. These agents target genetically normal endothelial cells that proliferate at a much higher rate during tumor angiogenesis compared with very low endothelial turnover rates in normal tissues (15). Antiangiogenic agents have been shown to increase therapeutic efficacy in conjunction with other chemotherapeutic agents and when used in combination with external radiotherapy (14). The $\alpha_v\beta_3$ integrin receptor, which binds several ligands via an RGD sequence (16), is expressed in normal vasculature (17) but is highly expressed in growing tumor vasculature (17–19), making it a potential target for antiangiogenic agents (19–21). High expression and activation of the $\alpha_v\beta_3$ integrin has also been correlated with the more metastatic and invasive breast tumors (22, 23). Inhibition of $\alpha_v\beta_3$ activity by mAb and cyclic RGD peptides has been shown to induce endothelial apoptosis (19), inhibit angiogenesis (18, 20), and increase endothelial monolayer permeability (24). The inhibition of $\alpha_v\beta_3$ activity has been associated with decreased tumor growth in breast cancer xenografts and melanoma xenografts (18, 25, 26). Synergy of cyclic RGD peptide with antibody interleukin-2 fusion protein has resulted in increased efficacy of therapy in murine models of melanoma, colon carcinoma, and neuroblastoma (27). Selective tumor uptake has been demonstrated with radiolabeled cyclic RGD peptides (28, 29).

Our laboratory recently demonstrated up to 50% increased tumor uptake of ^{90}Y-labeled DOTA-peptide-ChL6 mAb after treatment with the cyclic RGD peptide EMD 270179 cyclo arg-gly-asp-D-Phe-1-amino cyclohexane carboxylic acid (RGDf-ACHA) in nude mice bearing HBT 3477 breast cancer xenografts (30). On the basis of these initial results and results demonstrating efficacy of cyclic RGD peptide in some other tumor models (25, 27), we hypothesized that Cilengitide, combined with RIT, could act synergistically in inhibiting tumor growth in the HBT 3477 breast cancer tumor model. We tested

Received 2/11/02; accepted 6/4/02.

The costs of publication of this article were defrayed in part by the payment of page charges. This article must therefore be hereby marked *advertisement* in accordance with 18 U.S.C. Section 1734 solely to indicate this fact.

[1] Supported by NIH Grant PO1 CA-47829 from the National Cancer Institute (Bethesda, MD) and the Department of Energy Grants DEFG01-OONE22944 and DEFG03-84ER60233).

[2] To whom requests for reprints should be addressed, at Molecular Cancer Institute, 1508 Alhambra Boulevard, Suite 3100, Sacramento, CA 95816. Phone: (916) 734-3787; Fax: (916) 451-2857; E-mail: sjdenardo@ucdavis.edu.

[3] The abbreviations used are: RIT, radioimmunotherapy; CMRIT, combined modality RIT; RGD, Arg-Gly-Asp; mAb, monoclonal antibody; DOTA, 1,4,7,10-tetraazacyclododecane-*N*,*N*′,*N*″,*N*‴-tetraacetic acid; ChL6, chimeric L6; CAE, cellulose acetate electrophoresis; TUNEL, terminal deoxynucleotidyl transferase-mediated dUTP nick end labeling; DAPI, 4,6-diamidino-2-phenylindole; VEGF, vascular endothelial growth factor; VEGFR, VEGF receptor.

this hypothesis by treating HBT 3477 tumor bearing mice with Cilengitide and RIT. Cilengitide [cyclo (Arg-Gly-Asp-D-Phe-[Nme]-Val)] has even higher affinity for the $\alpha_v\beta_3$ receptor than does the RGD peptide EMD 270179 (31), and has demonstrated efficacy in melanoma tumor models as a single agent (25). Our results indicate that the combination of the antiangiogenic agent Cilengitide with RIT significantly increased efficacy and tumor and endothelial cell apoptosis without apparent increases in toxicity.

MATERIALS AND METHODS

Methods

Reagents. Carrier-free yttrium-90 (^{90}Y; Pacific Northwest National Laboratory, Richland, WA, or New England Nuclear, Boston, MA) was purchased as chloride in 0.05 M HCl. ChL6, a human-mouse antibody chimera (Bristol-Myers Squibb Pharmaceutical Research Institute, Seattle, WA), reacts with an integral membrane glycoprotein highly expressed on human breast, colon, ovary, and lung carcinomas (32–35). Cilengitide [cyclo Arg-Gly-Asp-D-Phe-(N-methyl)-Val; EMD 121974] is an antagonist selective for $\alpha_v\beta_3$ and $a_v\beta_5$ integrins, with IC_{50} values in the low nanomolar range for isolated $\alpha_v\beta_3$ integrins and in the low micromolar range for $\alpha_v\beta_3$-expressing M21 melanoma cells (30). Peptide synthesis and characterization were performed as described previously (31).

Cell Lines. HBT 3477, a human breast adenocarcinoma cell line, was obtained from Bristol-Myers Squibb Pharmaceutical Research Institute. Greater than 70% of HBT 3477 cells stain intensely with L6 (36). In HBT 3477 cells, bcl-2 is expressed and p53 is mutant, with a nonsense mutation in exon 10, resulting in a deletion in the region of the p53 protein that functions in tetramerization and in detection of double-stranded DNA breaks (37). HBT 3477 cells express functional $\alpha_v\beta_5$ integrin, but not $\alpha_v\beta_3$ integrin, because attachment to vitronectin is blocked by $\alpha_v\beta_5$-specific P1F6 antibody but is not blocked by $\alpha_v\beta_3$-specific LM609 antibody. Cilengitide blocks the attachment of HBT 3477 cells to vitronectin with an IC_{50} of $\sim$5 μM.[4]

^{90}Y-Labeled DOTA-peptide-ChL6. ChL6 was conjugated to DOTA and radiolabeled with ^{90}Y as described previously (11, 38, 39), with $\geq$80% efficiency to prepare ^{90}Y-labeled DOTA-peptide-ChL6. ^{90}Y-labeled DOTA-peptide-ChL6 was examined for structural and functional integrity by molecular sieving high-performance liquid chromatography (HPLC), CAE, and HBT 3477 cell-binding RIA (38). HPLC and CAE indicated that >90% of ^{90}Y-labeled DOTA-peptide-ChL6 was in monomeric form with less than 4% high molecular weight species as determined by CAE. Immunoreactive binding to live cells indicated a >92% reactivity. It was given as a single dose of 200, 230, or 260 μCi ^{90}Y-labeled DOTA-peptide-ChL6. Two hundred sixty μCi was chosen for the high-dose RIT studies, because previous studies in our laboratory had demonstrated efficacy in the HBT3477 tumor model at this dose level, typically with 100% response of tumors with few cures and deaths, making this the practical maximum tolerated dose (11). For the low-dose RIT studies, 200 μCi was chosen based on a previous study in which 230 μCi ^{90}Y-labeled DOTA-peptide-ChL6 resulted in few cures or complete responses but mostly partial responses (11).

Mice. Female (7–10-week old), athymic BALB/c *nu/nu* mice (Harlan Sprague Dawley, Inc., Frederick, MD) were maintained according to University of California animal care guidelines. HBT 3477 cells (3.0×10^6), harvested in log phase, were injected s.c. into one side of the abdomen for therapy studies (except where noted) and into both sides for immunopathology studies. Injection of RIT was by tail vein and Cilengitide was delivered by i.p. injection. "Day 0" was designated as the time of RIT injection or, for first RGD injection, for RGD-only group (40). Mice were killed by cervical dislocation for immunopathology studies at the times indicated, when tumor burden exceeded allowed limits, or at 84 days for therapy studies. The 84-day period was used because it allows sufficient time for accurate characterization of HBT 3477 tumor response to RIT and had been the standard time period used for the other RIT HBT3477 therapy studies in this laboratory to which these studies were compared (1, 11).

[4] Simon Goodman, Merck KGaA Darmstadt, unpublished observations.

Study Designs

No-RIT-Treatment Groups. Groups consisted of mice receiving no treatment (24 mice, 14 mice bearing two tumors each and 10 mice bearing one tumor); unlabeled ChL6 antibody (315 μg; 8 mice bearing two tumors each); and Cilengitide, given in six doses of 250 μg on days 0, 2, 4, 6, 8, and 10 (18 mice, each with one tumor).

High-Dose RIT-Treatment Groups. Groups consisted of mice receiving RIT as a single agent [260 μCi ^{90}Y-labeled DOTA-peptide-ChL6, (39 mice, 15 bearing two tumors each and 24 bearing one tumor)]; and RIT (260 μCi ^{90}Y-labeled DOTA-peptide-ChL6) combined with Cilengitide in six doses of 250 μg, starting on day 0, 1 h prior to RIT, followed by five more doses on days 2, 4, 6, 8, and 10 (42 mice, all with one tumor each). The Cilengitide dose of 250 μg was chosen based on data showing the biological effect on tumor cells in mice with no toxicity at a similar dose delivered by osmotic pump over 24 h (27), or delivered i.p. as single doses 3–5 times/week (25).

Low-Dose RIT-Treatment Groups. Groups consisted of mice receiving RIT as a single agent [200–230 μCi ^{90}Y-labeled DOTA-peptide-ChL6, (28 mice, including 9 bearing two tumors each from a previous study, which received 230 μCi ^{90}Y-labeled DOTA-peptide-ChL6, and 19 mice bearing one tumor each, treated with 200 μCi ^{90}Y-labeled DOTA-peptide-ChL6)]; and RIT (200 μCi ^{90}Y-labeled DOTA-peptide-ChL6) combined with Cilengitide in six doses of 250 μg starting on day 0, 1 h prior to RIT, followed by five more doses on days 2, 4, 6, 8, and 10 (30 mice, all with one tumor each).

Tumoricidal Effect. Tumors were measured with calipers in three orthogonal diameters three times a week. Tumor volume was calculated using the formula for hemiellipsoids (41). Initial tumor volume was defined as the volume on the day before treatment. Tumors that completely regressed were considered to have a volume of zero. Tumor responses were categorized as follows: cure (C), tumor disappeared and did not regrow by the end of the study (84 days); complete regression (CR), tumor disappeared for at least 7 days, but later regrew; partial regression (PR), tumor volume decreased by 50% or more for at least 7 days but then regrew; nonresponsive (NR), tumor volume decreased less than 50%. For mice bearing two tumors with differing responses, tumor response was described according to both tumor responses. Mice dying prior to 30 days from toxicity were excluded from tumor response results.

Toxicity. Weights and blood counts were measured two to three times per week for 12 weeks postinjection or until death. Blood samples were collected from tail veins using 2-μl microcapillary pipettes. Samples from mice within a dose group were pooled, and diluted 1:200 in PBS [PBS, 0.9% saline/10 mM sodium phosphate (pH 7.6)] for RBC counts; 1:100 in 1% (w/v) ammonium oxalate for platelet counts; or 1:20 in 3% (w/v) acetic acid for WBC counts (42).

Cellular Immunopathology Groups. Unless otherwise noted, groups consisted of two mice, each bearing two tumors, for a total of four tumors analyzed at each time point. The groups consisted of mice receiving no treatment (four mice, seven tumors); 250 μg Cilengitide, given as single dose followed by sacrifice at 2 h, 6 h, and 1–5 days after peptide injection; RIT only (260 μCi ^{90}Y-labeled DOTA-peptide-ChL6) followed by sacrifice at 2 h, 6 h, and 1–6 days (three mice, five tumors at 5 days); and RIT (260 μCi ^{90}Y-labeled DOTA-peptide-ChL6) combined with Cilengitide (250 μg) given 1 h prior to RIT, and repeated every other day through 10 days, followed by sacrifice at 2 h, 6 h, and 1–6 days after RIT. The tumors were removed, cut in half, frozen in optimal cutting temperature (O.C.T.) medium, and stored at $-$70°C until sectioning (10-μm sections). All of the time points were evaluated for apoptosis by TUNEL analysis (43), and selected time points (untreated, 1, 5, and 6 days) were assessed for differences in proliferation rate (Ki67) and microvessel density (CD31).

TUNEL Analysis of Total and Endothelial Apoptosis. Tumors were cut into 10-μm sections onto Fisher superplus slides (Fisher, Pittsburgh, PA), air-dried for 1 h and frozen at $-$70°C until TUNEL analysis with ApopTag Red kit (rhodamine used as label, Intergen, Purchase, NY) following the manufacturer's instructions subsequent to fixation for 10 min in 1% paraformadehyde. After TUNEL, the slides were rinsed and incubated overnight at 4°C with a rat antimouse mAb against CD31 at 1:100 dilution (PharMingen, San Diego, CA) to identify endothelial cells. Slides were rinsed and incubated for 1 h with an antirat antibody linked to FITC (1:50 dilution; PharMingen). Slides were rinsed, dipped briefly in DAPI (0.2 μg/ml) for background nuclear

Table 1 *Response of HBT Human Breast Cancer Xenografts to Combined Therapy with ^{90}Y-DOTA-Peptide-ChL6 and Cilengitide*

The efficacy of therapy was enhanced in CMRIT mice compared with mice treated with RIT or Cilengitide alone. Tumor responses shown indicate the number of responders in each category, based on the tumor response in mice surviving beyond 30 days. Mice that died from toxicity were excluded from tumor response results. No mice were euthanized for tumor burden prior to 30 days and no mice were excluded from tumor response results for this reason. Responses were categorized as cure (C, tumor disappeared and did not reappear before the end of the 84-day study); complete regression (CR, tumor disappeared for at least 1 week, but reappeared before the end of the study); partial regression (PR, tumor volume decreased by ≥50%); and nonresponsive (NR, tumor volume decrease was [<] 50%).

Treatment	Cilengitide	^{90}Y-DOTA-ChL6 (μCi)	Mice	C	CR	PR	NR
Control groups[a]							
No treatment			24	2	0	1	21
ChL6, 315 μg			8	1	0	0	7
Treatment groups							
Cilengitide	250 μg × 6		18	0	0	0	18
RIT (low dose)[b]		200–230	20	4	4	9	3
RIT (high dose)[c]		260	26	4	2	20	0
CMRIT (low dose)	250 μg × 6	200	22	8	3	10	1
CMRIT (high dose)	250 μg × 6	260	19	10	3	5	1
RIT (combined)[d]		200–260	46	8	6	29	3
CMRIT (combined)	250 μg × 6	200–260	41	18	6	15	2

[a] Mice bearing two tumors with differing responses from the control groups were categorized by the tumor with the lesser response (*e.g.*, a mouse with 1 PR and 1 CR tumor would be called a PR). If the best response is used for 2-tumored animals, outcomes affected read: No treatment CR 1, PR 3, NR 18; ChL6 C 2, NR 6; RIT (low dose) C 5, PR 11, NR 0; RIT (high dose) CR 6; PR 16; RIT (combined) C 9, CR 10, PR 27, NR 0.

[b] RIT low dose consisted of 315 μg ^{90}Y-DOTA-peptide-ChL6 radiolabeled with 200–230 μCi ^{90}Y. All of the combined-therapy mice in this group received 200 μCi, but some RIT-only mice received 230 μCi.

[c] RIT high dose consisted of 315 μg of ^{90}Y-DOTA-peptide-ChL6 radiolabeled with 260 μCi ^{90}Y.

[d] Combined results are included for overall comparison of CMRIT versus RIT responses and represent the sum of the mice in both the low- and high-dose studies.

stain, rinsed again, and mounted, followed by storage in the dark at 4°C until quantitation.

Quantitation of Total Apoptosis and Endothelial Apoptosis. An Olympus microscope equipped with a Chroma Pinkle Filter Set (Chroma, Brattleboro, VT) with excitation filters for UV, FITC and Rhodamine and dual/triple bandpass filters to allow simultaneous viewing of multiple wavelengths, was used to quantify six randomly chosen ×600 fields (150,000 μm^2/field) in nonnecrotic regions of each section. Fields were chosen to cover the entire viewing area using a DAPI label, which typically included 300–350 cells. Total apoptosis was determined by the average number of positive nuclei per field for each tumor, whereas endothelial apoptosis was determined using the same fields with a dual bandpass filter to count cells labeled by both FITC (CD31) and rhodamine (TUNEL). Fields were chosen from apparently non-necrotic areas of tumor sections, because HBT 3477 xenografts typically grow quickly in nude mice, doubling their volumes in 6 days (11), which results in central necrosis of untreated tumors. Because TUNEL may label necrotic cells, although less intensely (44, 45), this strategy was chosen over a completely random process.

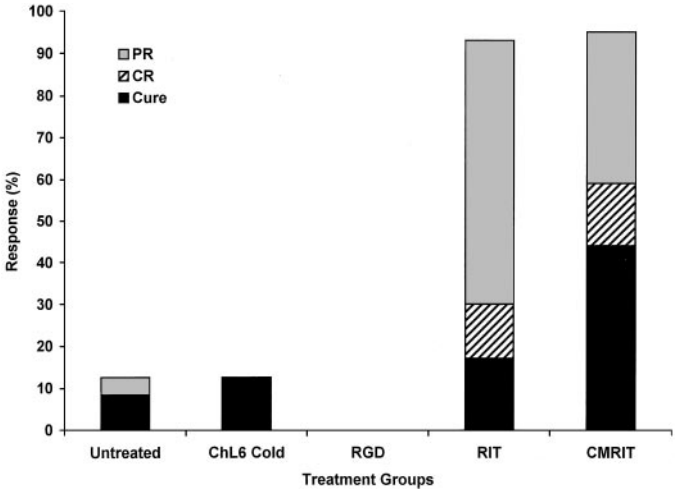

Fig. 1. Increased efficacy of treatment in mouse breast cancer xenografts is obtained with CMRIT. Tumor responses to ^{90}Y-labeled DOTA-peptide-ChL6 and Cilengitide used as single agents and in combined therapy. Results illustrate combined high-dose and low-dose results for RIT (200–260 μCi ^{90}Y-labeled DOTA-peptide-ChL6) using worst outcome for 2-tumored mice. Groups were: untreated, mice treated with 315 μg of unlabeled ChL6, mice treated with six doses of 250 μg of Cilgengitide, mice treated with RIT alone, and CMRIT mice treated with six doses of 250 μg of Cilengitide and one dose of RIT (200 and 260 μCi). Responses were assessed at the end of 84 days. Significantly increased efficacy of treatment was observed in CMRIT mice compared with RIT mice (Fisher Exact for best outcome of 2-tumored mice, $p = 0.02$). *PR*, partial regression; *CR*, complete regression.

Proliferation and Microvessel Density Analyses. Ten-μm sections of tumors from untreated and mice treated with RGD, RIT, and CMRIT, and killed at 1, 5, and 6 days after treatment, were fixed for 10 min in ice-cold acetone, rinsed in PBS, and briefly incubated in methanol with 0.6% H_2O_2 (5 min). After rinsing in PBS, sections were blocked for 10 min with 10% goat serum and 1% BSA in PBS. Mouse anti-Ki67 mAb (PharMingen, clone B56) was applied in blocking solution (6.25 μg/ml) and the slides were incubated at room temperature for 2 h, followed by rinsing in PBS. Goat antimouse rhodamine-labeled or goat antimouse Cy-3-labeled antibody was applied (Jackson ImmunoResearch Laboratories, Inc., West Grove, PA; 1:100) and the slides were incubated for 1 h at room temperature. After a rinsing in PBS, the sections were incubated for 1 h at room temperature with rat antimouse CD31 antibody (PharMingen, 1:100), followed by a rinsing in PBS and a subsequent 1-h incubation with goat antirat FITC-labeled antibody (PharMingen, 1:50). After rinsing in PBS, the slides were counterstained with DAPI (0.4 μg/ml) and mounted in Biomeda gel mount (Fisher) under coverslips. Quantitation of Ki67 was performed using an Olympus microscope at ×1000 magnification for an assessment of proliferation. The mean total number of Ki67-positive cells/field in a tumor was determined by counts from six fields per tumor chosen randomly by DAPI stain. Microvessel density was determined by counting the number of CD31-stained vessels per random field at ×400 magnification. Any endothelial cell or cell cluster that was positive for CD31 and that was separate from an adjacent cluster was counted as one microvessel (46). Six randomly chosen fields per tumor section were used to establish an average for each tumor (47). Average microvessel density for a treatment group was determined by averaging the values from four tumors/group.

β_3 and CD31 Expression by HBT 3477 Tumors in Nude Mice. Tumors were cut in half, frozen in O.C.T. medium (Tissue Tek; Miles, Inc., Elkhart, IN) and stored at –70°C until sectioning. Ten-μm sections were air-dried and frozen at −70°C until stained. Sections were then fixed in ice-cold acetone for 10 min, rinsed in PBS, and blocked in 10% goat serum in PBS for 30 min. Hamster antimouse CD61 (β3) mAb (PharMingen) was applied at 10 μg/ml and the slides were incubated for 3 h at room temperature. After rinsing in PBS, antihamster rhodamine-linked antibody (Jackson ImmunoResearch Laboratories, Inc.) was applied (1:50), followed by a 1-h incubation at room temperature. After rinsing in PBS, rat antimouse CD31 antibody was applied (1:100; PharMingen) and the slides were incubated for 1 h at room tempera-

ture. After PBS rinsing, antirat FITC-linked antibody (1:50; PharMingen) was applied, and the slides were incubated for 1 h at room temperature and rinsed in PBS. The slides were dipped in DAPI (0.2 μg/ml) and mounted with Biomeda gel mount (Fisher) under coverslips. Coexpression of β_3 and CD31 was observed with an Olympus microscope equipped with a Chroma Pinkle Filter Set (Chroma, Brattleboro, VT) with excitation filters for UV, FITC, and rhodamine, and dual/triple bandpass filters to allow simultaneous viewing of multiple wavelengths.

Statistical Analysis. Statistical analysis of mortality data for RIT and CMRIT mice was performed using a Fisher exact test with StatExact software to determine whether mortality was different. Statistical analysis of therapy data were done using a Cochran Mantel Haenszel test to evaluate the effect of the RIT dose on outcome for RIT and CMRIT groups. A comparison of cure rates compared with all of the other responses for RIT *versus* CMRIT groups was done by the Fisher exact test, in the best tumor response used for 2-tumored animals. Statistical differences between immunopathology groups at the different time points were assessed by ANOVA (Fisher protected least significant difference PLSD) using STATview software as appropriate, with $P < 0.05$ considered significant.

RESULTS

Tumoricidal Effect. Most of the tumors in untreated mice, mice receiving Cilengitide alone, and mice receiving ChL6-unlabeled antibody grew without interruption. No apparent effect of Cilengitide (6 $\times$ 250 μg doses total, given every other day) was observed on tumor growth, resulting in no cures in 18 mice tested. Two mice receiving unlabeled ChL6 antibody in addition to two untreated mice experienced spontaneous regression of their tumors, leading to a 8% (3/50) cure rate for non-RIT mice (Table 1; Fig. 1). Mice receiving RIT were treated with 260 μCi (high dose) or 200–230 μCi (low dose) ^{90}Y-labeled DOTA-peptide-ChL6, by itself or in combination with six doses of Cilengitide. Tumor responses in mice dying from toxicity prior to 30 days after RIT were excluded from efficacy assessment. High-dose RIT alone resulted in four cures in 26 mice (15%), whereas low-dose RIT alone resulted in five cures in 20 mice (25%). CMRIT with low-dose RIT resulted in 8 cures in 22 mice ($p = 0.514$), whereas CMRIT with high-dose RIT resulted in 10 cures in 19 mice ($p = 0.011$). Statistical analysis indicated that there was not a difference in outcome of therapy based on RIT dose adjusted for RIT or CMRIT. As the outcome was not altered by the dose ($P > 0.8$), outcomes for RIT were compared with outcomes for CMRIT. Our results show that CMRIT resulted in significantly more cures (44% cure rate) than RIT (20% cure rate; $P = 0.020$), consistent with increased efficacy of CMRIT over RIT alone.

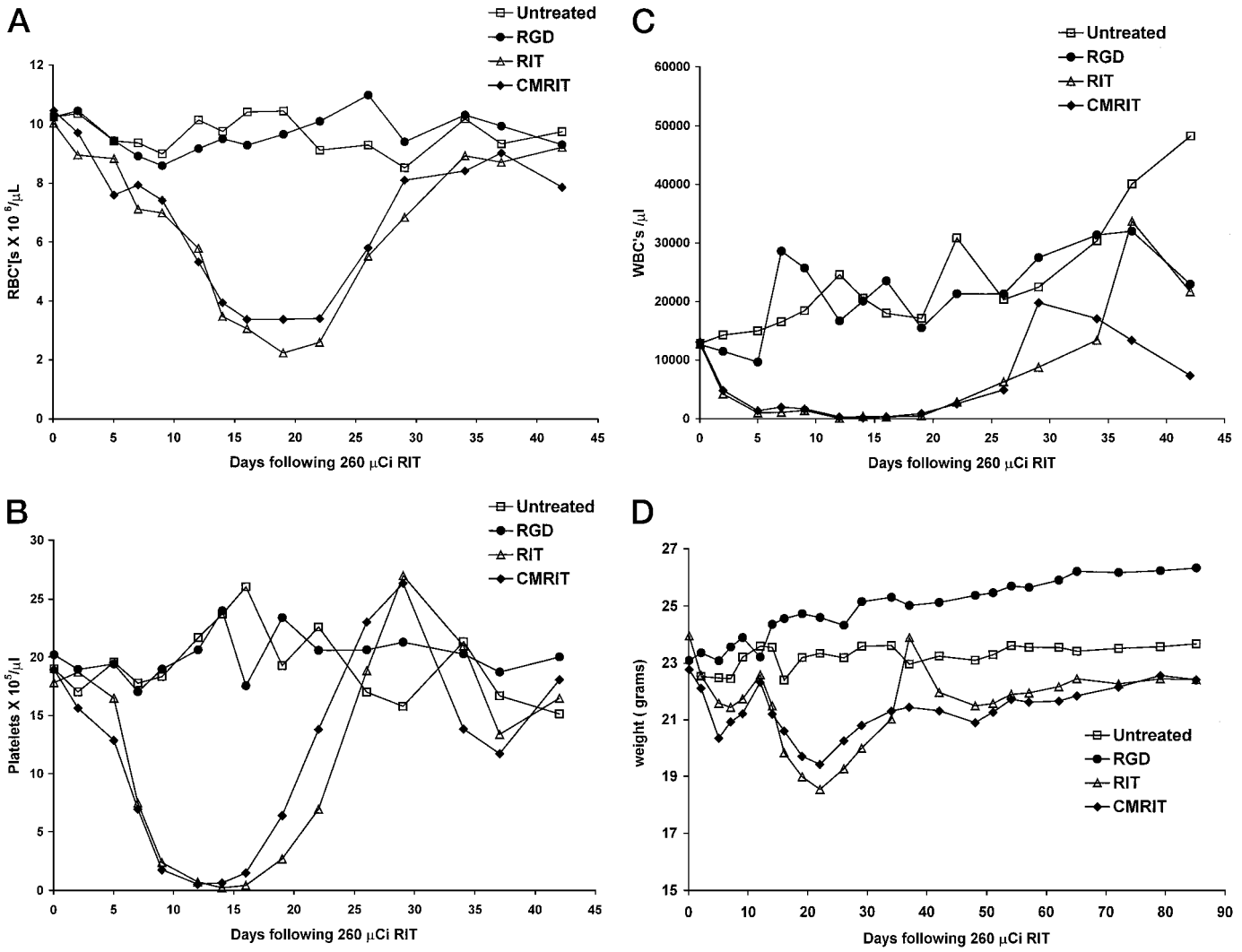

Fig. 2. Cilengitide therapy or CMRIT does not increase toxicity. (*A*) RBCs, (*B*) platelets, (*C*) WBCs, and (*D*) mouse weights for groups of untreated mice (5), mice treated with Cilengitide (six doses of 250 μg) alone (13), mice treated with RIT alone (260 μCi ^{90}Y-labeled DOTA-peptide-ChL6; (5), and mice treated with CMRIT (260 μCi ^{90}Y-labeled DOTA-peptide-ChL6 and six doses of 250 μg Cilengitide; (13) from a single trial. Results shown represent pooled blood samples for each group and average weights $\pm$ SE for each group on days shown. Cilengitide by itself or in combination with RIT did not increase toxicity.

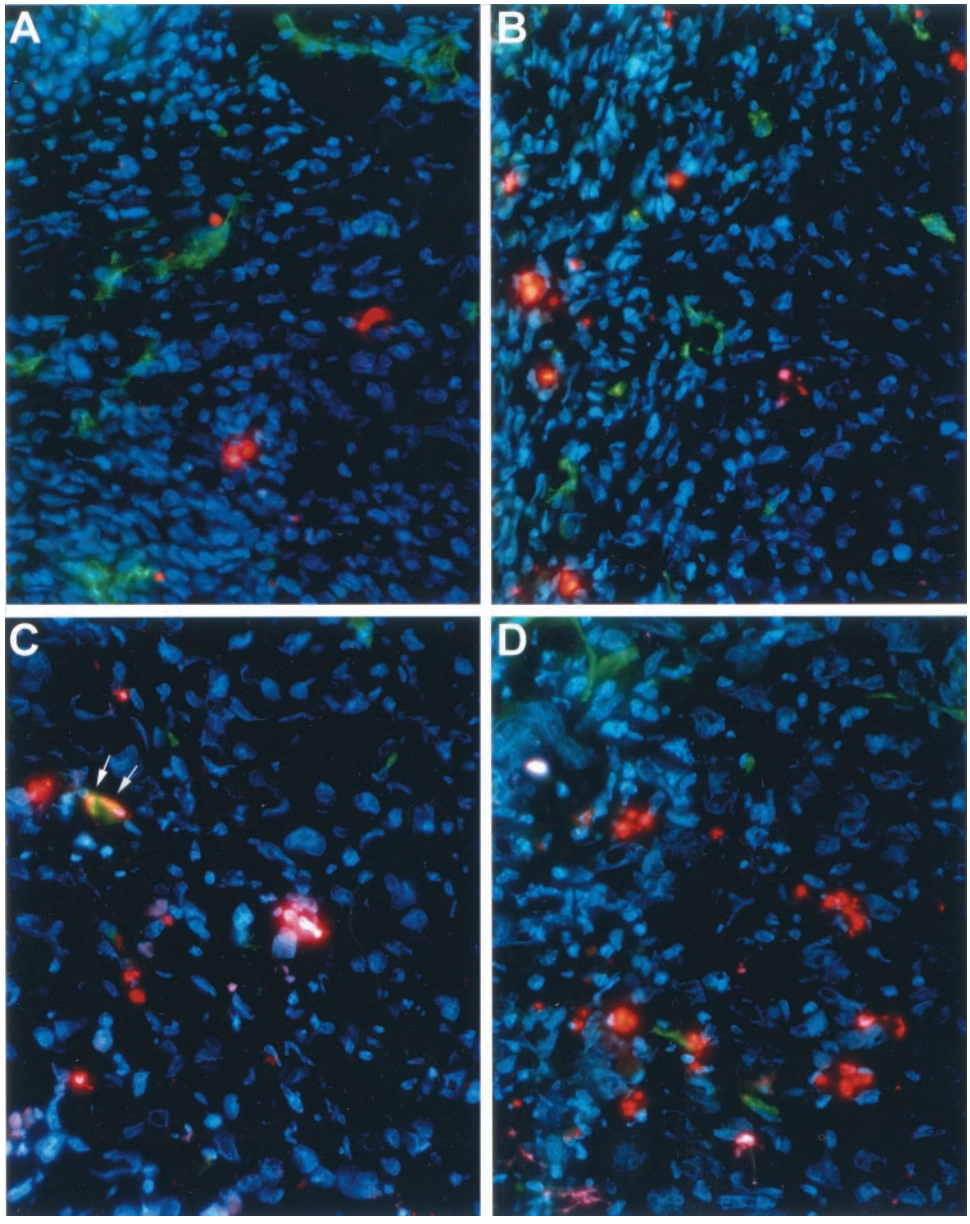

Fig. 3. CMRIT results in increased apoptosis. Apoptosis (TUNEL with ApopTag Red) and CD31 (FITC) in 10-μm sections of tumors from: (*A*) untreated; (*B*) RGD-treated (one dose, 250 μg of Cilengitide; (*C*) RIT (260 μCi ^{90}Y-labeled DOTA-peptide-ChL6); and (*D*) CMRIT (260 μCi ^{90}Y-labeled DOTA-peptide-ChL6 and 6 doses of 250 μg of Cilengitide) mice assessed 5 days after the start of treatment. Apoptosis (rhodamine) is observed in tumor cells and in endothelial cells (FITC), in which rhodamine and FITC dyes are colocalized (*orange cells marked by arrowheads*). Background nuclear stain obtained with DAPI. Sections photographed at $\times$600 with an Olympus microscope equipped with Pinkle filters. Increased apoptosis of tumor and endothelial cells was observed in CMRIT mice compared with mice treated with RIT alone (ANOVA, $P < 0.05$).

Toxicity of Cilengitide. No increased mortality or toxicity was induced by Cilengitide (250 μg, six doses over 10 days) alone compared with untreated mice [no mice died from toxicity in any of the groups that did not receive RIT (untreated, unlabeled ChL6, or Cilengitide)]. Cilengitide-treated and untreated mice displayed similar weight changes and RBC, WBC, and platelet levels. Mice treated with either high- or low-dose RIT and mice treated with the combination of RIT and Cilengitide demonstrated decreased weight, RBC, WBC, and platelet counts compared with mice receiving no RIT, but the combination of RIT with Cilengitide did not depress these values beyond those observed with RIT alone (Fig. 2, *A–D*). At the high dose of RIT, mortality was higher than in untreated mice in both RIT [13 (33%) of 39 mice] and CMRIT [23 (55%) of 42 mice] groups, but mortality was not statistically increased by CMRIT (Fisher exact test, $P = 0.0736$). Likewise, mortality was increased in low-dose RIT and CMRIT groups over untreated mice, but the mortality of CMRIT [8 (27%) of 30 mice] was not increased above RIT (8 (29%) of 28 mice; Fisher's exact test, $P = 1.000$]. When low- and high-dose mortality results are combined, CMRIT does not result in increased mortality over RIT (Fisher's exact test, $P = 0.1652$). These results indicate that Cilengitide, administered alone or in combination with RIT, does not significantly increase toxicity.

Apoptosis in Tumor and Endothelial Cells (Total Cells). Apoptosis was assessed by the TUNEL method (43) in combination with CD31 staining to identify endothelial cells (Fig. 3). The number of TUNEL-positive tumor and endothelial cells (total cells) were averaged per tumor from six random fields ($\times$600) of nonnecrotic tissue, chosen such that cells covered the entire area of the field, with an average of approximately 350 cells/field. Untreated tumors had an average of 9 $\pm$ 1.0 positive cells/field (2.6%). A single dose of Cilengitide significantly increased apoptosis 1 day after treatment [16.2 $\pm$ 1.89 (4.6%)], but this level of apoptosis subsequently decreased. Compared with untreated tumors, RIT alone resulted in significantly increased apoptosis (as noted on Fig. 4), with the greatest number of apoptotic cells seen at 6 days [21.4 $\pm$ 2.9 (6.1%)]. Apoptosis after CMRIT was higher than in all of the other treatment groups at all time points except at 6 days [significantly increased apoptosis noted (Fig. 4)]. Apoptosis after CMRIT peaked at 5 days

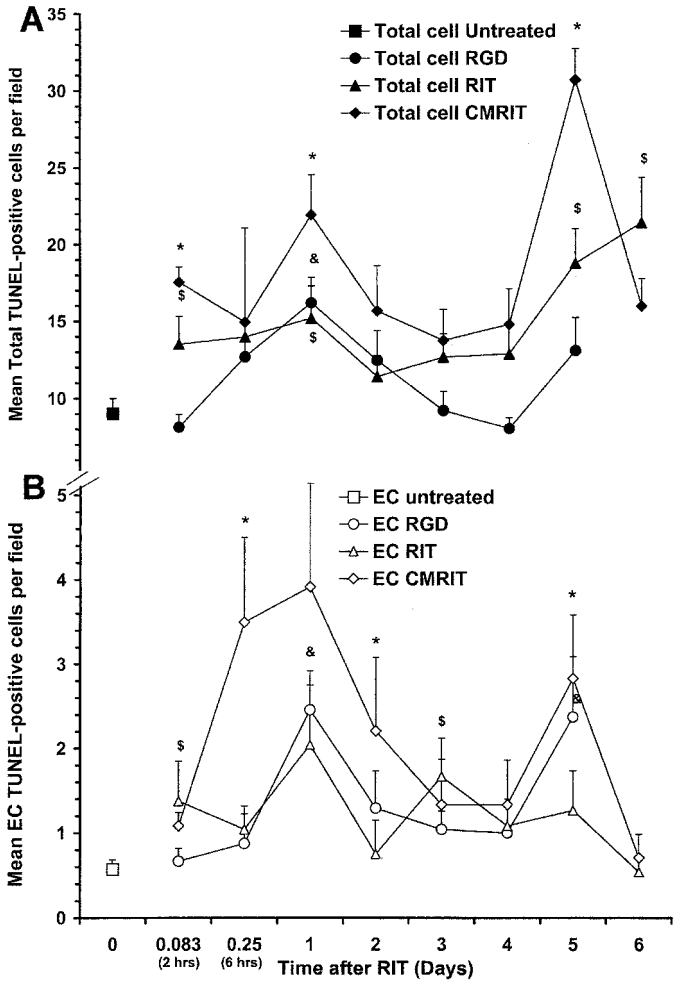

Fig. 4. Cilengitide results in increased apoptosis in tumor and endothelial cells at 1 and 5 days after Cilengitide or CMRIT. *A*, Apoptosis in total cells (*closed symbols*) and (*B*) endothelial cells (*EC*; *open symbols*) was assessed by TUNEL and CD31 immunohistochemical analysis in HBT 3477 tumors from untreated mice (■); mice treated with RGD [one dose, 250 μg of Cilengitide (●)]; mice treated with RIT [260 μCi ^{90}Y-labeled DOTA-peptide-ChL6 (▲)]; and mice treated with CMRIT [260 μCi ^{90}Y-labeled DOTA-peptide-ChL6 and six doses of 250 μg of Cilengitide (♦)]. Apoptosis was quantitated at ×600 magnification from six random fields per tumor, with four tumors used for the determination of the treatment mean. *Error bars*, SE; ∗, CMRIT values significantly greater (ANOVA, $P < 0.05$) than RIT values; &, RGD values significantly greater than untreated values (ANOVA, $P < 0.05$); $, RIT values significantly greater than untreated values. Total-cell apoptosis for CMRIT tumors was significantly different from that in RIT tumors at 2 h, 1 day, and 5 days after RIT. Endothelial apoptosis was significantly increased in CMRIT mice over RIT mice at 6 h, 2 days, and 5 days after RIT. *X* axis was not drawn to scale to illustrate changes at early time points. *Break in Y axis*, change of scale between total-cell apoptosis and EC apoptosis.

after RIT [30.7 ± 2.0 cells/field (8.8%)], with a lower peak at 1 day after CMRIT [21.9 ± 2.6 (6.3%)]. These two peaks of apoptosis are consistent with two "waves" of apoptosis occurring. However, the difference in total cell apoptosis occurring in CMRIT tumors compared with RIT tumors is additive and, thus, suggests that other mechanisms may also affect efficacy.

Endothelial Apoptosis. Because RGD peptide had previously been shown to induce apoptosis in vascular endothelial cells (19), we first compared endothelial apoptosis in Cilengitide-treated (single dose) tumors with untreated tumors. Significantly increased apoptosis was observed 1 day (2.5 ± 0.5) and 5 days (2.4 ± 0.7) after RGD treatment compared with untreated tumors (0.6 ± 0.1). However, these differences in apoptosis between RGD-treated and -untreated tumors were not reflected by differences in growth or tumor volume even with multiple (6) doses of Cilengitide. RIT-alone also resulted in significantly increased endothelial apoptosis compared with untreated tumors at early time points (Fig. 4). CMRIT was associated with two peaks of endothelial cell apoptosis, at 1 day and 5 days after RIT, with the highest levels at 1 day (3.9 ± 1.2 cells/field). (Fig. 4). The average level of endothelial apoptosis in CMRIT tumors was higher than all of the other groups at all times, except at 3 days and 6 days. However, increased endothelial apoptosis did not appear to precede total-cell apoptosis in CMRIT tumors, with peaks occurring both at 1 day and at 5 days.

Total Cell Proliferation. The average number of Ki67-positive cells was determined for untreated tumors and for tumors at 1, 5, and 6 days (RGD-alone was not done for 6 days). Ki67 antibody recognizes protein present in the nuclei of proliferating cells at all of the active stages of cell cycle but does not recognize protein found in cells at G_0 (48, 49). Our results indicate that RIT-alone or RGD-alone significantly decreased proliferation rates of cells active in cell cycle at 5 days compared with rates in untreated mice (Table 2). CMRIT similarly decreased proliferation compared with untreated mice and resulted in significantly decreased proliferation at 6 days compared with RIT-alone (Fig. 5).

Microvessel Density. Microvessel density for each tumor was determined by averaging the total number of noncontiguous, CD31-stained regions in six randomly chosen fields from one section of each tumor from untreated mice, RGD-treated, and RIT-and-CMRIT-treated mice at key time points after treatment (Table 2). Significantly decreased microvessel density compared with untreated mice was observed 6 days after RIT in mice receiving either RIT alone or RIT combined with Cilengitide. Increased endothelial apoptosis (above that with RIT) observed during day 1 and at day 5 did not appear to be associated with measurable differences in microvessel density and did not precede total-cell apoptosis. These data indicate that increased endothelial apoptosis associated with CMRIT may contribute to, but is not likely to be the only mechanism affecting, the therapeutic outcome. In addition, the data through day 6 do not indicate that decreased microvessel counts explain the difference in therapeutic outcome between RIT and CMRIT.

Expression of $\alpha_v\beta_3$ on HBT 3477 Tumors. Immunohistochemistry with anti-β_3 antibody reactive with mouse integrin (CD61) demonstrated limited labeling of selected regions of HBT 3477

Table 2 *Effect of treatment on microvessel density and number of Ki67-positive cells*

CMRIT resulted in significantly decreased proliferation compared with RIT 6 days after the administration of RIT. No difference in the microvessel density between treatment groups was noted.

Day	Untreated	Cilengitide[a]	RIT[b]	CMRIT[c]
Microvessel density[d]				
0	16 ± 3			
1		12 ± 2	15 ± 1	15 ± 2
5		20 ± 4	13 ± 1	12 ± 1
6			9 ± 1[e]	9 ± 2[e]
Proliferating Cells[f]				
0	17 ± 1			
1		14 ± 2[f]	18 ± 1	19 ± 1
5		13 ± 1[f]	13 ± 1[f]	13 ± 1[f]
6			7 ± 1	3 ± 1[g]

[a] Cilengitide given as a single i.p. dose of 250 μg.
[b] RIT consisted of a single i.v. dose of 315 μg ^{90}Y-DOTA-peptide-ChL6 radiolabeled with 260 μCi ^{90}Y.
[c] CMRIT consisted of a single i.v. dose of 315 μg ^{90}Y-DOTA-peptide-ChL6 radiolabeled with 260 μCi ^{90}Y and four i.p. 250-μg doses of RGD peptide given on alternate days, starting 1 h prior to RIT.
[d] Microvessel density was determined as the average number ± SE of CD31-positive regions in six fields for each tumor counted at × 400.
[e] Significantly different from untreated (ANOVA, $P < 0.05$).
[f] The average number of proliferating cells was determined by taking the average number of Ki67-positive cells in six fields for each tumor counted at × 1000 (approximately 112 ± 10 cells/field).
[g] CMRIT significantly less than RIT (ANOVA, $P < 0.05$).

tumors in nude mice (Fig. 6). β_3-labeled regions included areas appearing as ring-like vascular structures, which were colabeled by an antibody recognizing CD31, which is consistent with $\alpha_v\beta_3$ expression in the blood vessels supplying these tumors. Substantially less expression of β_3 was observed than of CD31, which would be expected if only a small proportion of endothelial cells labeled by CD31 were neovascular.

DISCUSSION

Our results demonstrate that increased efficacy of treatment without increased toxicity can be achieved when RIT is combined with the $\alpha_v\beta_3$-specific Cilengitide, compared with single-modality RIT or Cilengitide therapy. CMRIT with high-dose RIT resulted in 53% cures compared with 15% cures for RIT alone, and 0% cures for Cilengitide alone, whereas combined-dose levels resulted in 44% cures compared with 20% cures for RIT alone. Although there were increased deaths associated with CMRIT at the higher-dose level, mortalities for CMRIT and RIT were not statistically different. These results indicate that significantly better outcome of therapy is associated with CMRIT compared with therapy with single agent, without an accompanying statistical increase in toxicity.

Synergy of radioimmunotherapy has been demonstrated with other antiangiogenic or chemotherapeutic agents in several tumor models (1, 12, 50–61). The combination of paclitaxel and radioimmunotherapy has proved effective in increasing cures or inhibiting tumor growth in breast (1, 58), prostate (59), and lymphoma (60) cancer models. mAb to epidermal growth factor receptor in combination with radioimmunotherapy also increased cures in the HBT 3477 breast cancer model (57) and in a squamous cell carcinoma model (56). Chemotherapeutic agents such as gemcitabine (52), topotecan (54), hypoxic cytotoxic agents (55), and combinations of chemotherapeutic agents (51) have demonstrated improved control of tumor growth over RIT-alone. The antiangiogenic agent 2-methoxyestradiol combined with an anticolorectal mAb improved efficacy over RIT-alone in mice bearing human colon cancer xenografts (50). Combined RIT with the antivascular agent combretastatin also improved therapeutic outcomes in colorectal xenografts (53). The combination of antivascular RIT delivered prior to tumor-targeting RIT demonstrated more homogeneous tumor uptake of tumor RIT (61). A number of other combined modality studies using external beam radiation with antiangiogenic agents have shown increased efficacy over radiation alone, including studies with angiostatin (62, 63), endostatin (64), TNP-470 (65, 66), anti-VEGF mAb (67, 68); anti-VEGFR-2 mAb (69), anti-VEGFR soluble receptors (70), VEGFR inhibitor PTK787/ZK222548 (71), and the antivascular agent NM-3 (72). The particular appeal of antiangiogenic agents is their potential to target a nonresistant population of cells without increased toxicity, making antiangiogenic agents promising for chronic therapy to prevent tumor cell recovery and metastasis (14).

The $\alpha_v\beta_3$ integrin receptor, targeted by Cilengitide, when bound to agonists such as vitronectin, fibronectin, and osteopontin, suppresses p53 and the bax cell death pathway (73). RGD cyclic peptides and mAbs that target and block the $\alpha_v\beta_3$ receptor induce apoptosis in endothelial cells, inhibit angiogenesis, and block tumor growth (18–20, 74). Cilengitide can inhibit the growth of medulloblastoma and glioblastoma brain tumors in mice (75), as well as melanoma tumors in mice (25) through its blockade of the $\alpha_v\beta_3$ receptor. It is currently in clinical trials (Phase I/II anaplastic glioma and Phase I Kaposi's

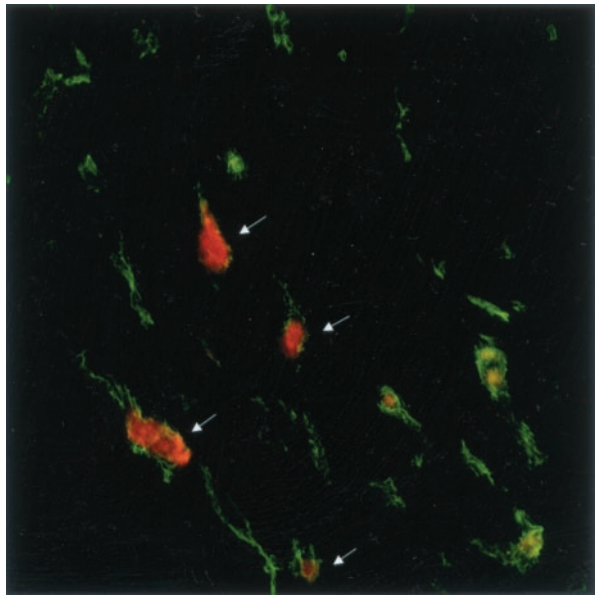

Fig. 6. β_3 and CD31 expression on HBT 3477 breast cancer tumor. The tumor removed from an untreated mouse was analyzed for expression of integrin β_3 and endothelial protein CD31 using immunohistochemical techniques. Hamster mAb to mouse β_3 was applied, followed by antihamster rhodamine-linked antibody. Subsequently rat antimouse CD31 mAb was applied followed by antirat FITC-linked antibody. Colocalization (*orange color*, *arrows*) of rhodamine (β_3) and FITC (CD31) is consistent with $\alpha_v\beta_3$ integrin expression in the blood vessels supplying the tumor. Tumor section was photographed at ×600 with an Olympus microscope equipped with Pinkle filters.

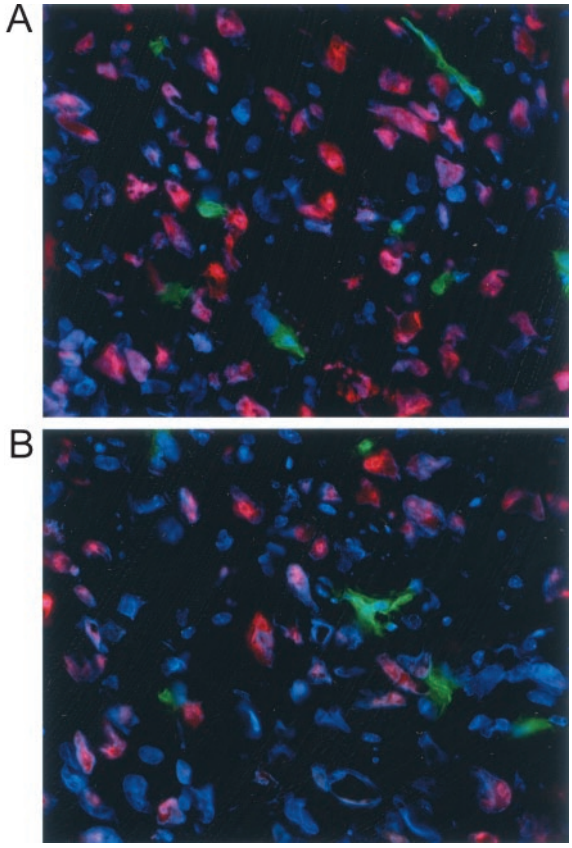

Fig. 5. Decreased proliferation of tumor cells after CMRIT *versus* RIT. Proliferating cells in (*A*) RIT and (*B*) CMRIT tumors were identified on 10-μm frozen sections of tumors 6 days after RIT by Ki67 mouse mAb followed by anti-mouse rhodamine-linked antibody. Endothelial cell clusters used for microvessel density counts were identified by anti-CD31 rat mAb followed by antirat antibody linked to FITC. Nuclear stain was DAPI. Proliferation was quantitated at ×1000 magnification from six random fields per tumor, with four tumors used for the determination of the treatment mean. Fewer Ki67-positive cells were observed in CMRIT tumors compared with RIT tumors 6 days after RIT, although the number of microvessels was not different at this time point. Sections were photographed at ×600 with an Olympus microscope equipped with Pinkle filters.

sarcoma)[5] (76) with only mild side effects, including nausea, anorexia, fatigue, and malaise, with no bone marrow suppression and no dose-limiting toxicity reached when given as a twice-weekly continuous infusion of up to 850 mg/m^2 (76).

Because the combination of Cilengitide with RIT increased the percentage of mice cured of an aggressive, p53-mutant human breast cancer (37), we considered potential mechanisms that could account for this increase. Previous data demonstrated that 250 μg of RGD peptide (EMD 270179), provided 1 h before RIT, increased the uptake of RIT by HBT 3477 tumors up to 50% (30), which led to a consideration of whether increased tumor uptake of RIT could have resulted in increased cures. However, in a previous study of this HBT 3477 model using ^{90}Y-labeled DOTA-peptide-ChL6 at doses ranging from 110 μCi to 330 μCi, we found that increased cure rates did not follow increased injected doses above 260 μCi ^{90}Y-labeled DOTA-peptide-ChL6. These results strongly suggest that increased uptake of RIT associated with Cilengitide is not the major factor responsible for the increased cures.

As another mechanism, we investigated the vascular contribution to CMRIT by assessing endothelial apoptosis and its time course compared with tumor-cell apoptosis. If Cilengitide induced endothelial apoptosis and subsequently induced tumor cell apoptosis after the loss of endothelial cells, we would expect to observe increased endothelial apoptosis occurring prior to increased total cell apoptosis (77, 78). Cilengitide in combination with RIT elevated both endothelial and total-cell apoptosis levels above that observed with RIT at almost all time points, with significantly increased levels at 1 and 5 days. In addition, a single dose of Cilengitide significantly increased endothelial apoptosis at the same time points compared with untreated tumors. Although we did not detect a clear pattern of endothelial apoptosis preceding total cell apoptosis, there was a persistent elevation of endothelial apoptosis in CMRIT compared with RIT. However the effect of this difference was not reflected directly by differences in microvessel density at the time points assessed. It is possible that Cilengitide affected the quality of the microvascular organization, which would not have been reflected by the microvessel density (68). This is consistent with the decrease in proliferation observed at 6 days in CMRIT compared with RIT tumors, the latest time point evaluated, when the number of microvessels had decreased in both RIT and CMRIT tumors.

Other possible differences between CMRIT and RIT could be related to indirect inhibitory effects of Cilengitide. Radiation has been shown to induce the accumulation and activation of β_3 integrin on tumor blood vessels within 1–4 h of irradiation (79, 80). The increase is associated with platelet accumulation in the lumen of irradiated tumor vessels (79, 80). Platelet adhesion to endothelial cells has been inhibited by blockade with antibody to $\alpha_v\beta_3$ integrin (81), and platelets potentially contribute to tumor angiogenesis through growth factors contained in α-granules (82, 83). Cilengitide has been shown to have an IC_{50} of 420 nM for isolated $\alpha_{2b}\beta_3$ receptor, compared with 5 nM for $\alpha_v\beta_3$ (30). It is possible that Cilengitide, at this dosage in this mouse model, inhibited the accumulation of platelets in tumor vasculature in response to radiation and, thus, decreased the paracrine interaction with tumor cells. In addition, the $\alpha_v\beta_3$ integrin receptor has been shown to participate in the full activation of the VEGFR-2 (84). Inhibition by Cilengitide could interfere with downstream effects of the VEGFR-2 on endothelial cells, such as decreased growth factor release to adjacent tumor cells (85), which would lead to an overall inhibition of tumor cell proliferation.

Although Cilengitide altered HBT 3477 tumor growth only in combination with RIT, it has been effective at inhibiting tumor growth in medulloblastoma and glioblastoma tumors in mice (100 μg/day). Specifically, the peptide is effective in tumors implanted orthotopically in the brain but not in tumors implanted s.c. in the same mice (75). RGD peptide (250 μg/5x weekly) has also shown efficacy in inhibiting the growth of melanoma tumors when implanted s.c. in mice via direct inhibition of tumor cells (25). These data indicate that some tumors may be more sensitive to inhibition by this peptide, possibly because of increased sensitivity to ligand expression and blockade (75), differences in tumor cell expression of $\alpha_v\beta_3$ receptors (25), and differences in the activation level of receptors (23). The lack of responsiveness of HBT 3477 s.c. tumor growth to Cilengitide inhibition (single modality) likely indicates that, in this model, tumor growth uses existing blood vessels or that sufficient blood vessel growth occurs even in the presence of Cilengitide. After RIT, at a time when blood vessel density has decreased substantially, Cilengitide inhibition may lead to decreased tumor cell and endothelial cell recovery from radiation damage, resulting in increased tumor cell death in waves of apoptosis, related to increased therapeutic efficacy.

In conclusion, our results are consistent with the increased efficacy of RIT of breast cancer tumors resulting from combined treatment with the anti-$\alpha_v\beta_3$ peptide, Cilengitide. Although these results were obtained in a single model of breast cancer, the molecular biology of this tumor has been documented to be relevant to the sources of therapy failures in patients with metastatic breast cancer (36, 86). The therapeutic synergy is likely caused by the combined effects of several mechanisms, leading to increased apoptosis and decreased proliferation. The higher level of endothelial apoptosis observed with CMRIT treatment would, however, be consistent with endothelial loss impacting tumor cell loss, and contributing to the observed increase in cures. The enhanced therapeutic response achieved by the addition of the antiangiogenic agent, Cilengitide, to RIT is remarkable because the therapeutic synergy was achieved without additional toxicity, which indicates immense potential for Cilengitide specifically, and antiangiogenic agents in general, for combination therapy with RIT.

ACKNOWLEDGMENTS

The authors thank Dr. A. Joncyzk, Merck KGaA for the gift of Cilengitide, Dr. Simon L. Goodman, Merck KGaA Darmstadt for his thoughtful review and suggestions, and David L. Kukis, University of California at Davis Sacramento Medical Center, Sacramento, CA for his expert support in providing all radiolabeled material.

Prof. Matzku passed away on May 27, 2002.

REFERENCES

1. DeNardo, S. J., Kukis, D. L., Kroger, L. A., O'Donnell, R. T., Lamborn, K. R., Miers, L. A., DeNardo, D. G., Meares, C. F., and DeNardo, G. L. Synergy of Taxol and radioimmunotherapy with yttrium-90-labeled chimeric L6 antibody: efficacy and toxicity in breast cancer xenografts. Proc. Natl. Acad. Sci. USA, *94:* 4000–4004, 1997.
2. Harris, C. Structure and function of the *p53* tumor suppressor gene: clues for rational cancer therapeutic strategies. J. Natl. Cancer Inst. (Bethesda), *88:* 1442–1455, 1996.
3. Upadhyay, S., Li, G., Liu, H., Chen, Y. Q., Sarkar, F. H., and Kim, H. R. *Bcl-2* suppresses expression of p21$^{WAF1/CIP1}$ in breast epithelial cells. Cancer Res., *55:* 4520–4524, 1995.
4. Allred, D. C., Clark, G. M., Elledge, R., Fuqua, S. A., Brown, R. W., Chamness, G. C., Osborne, C. K., and McGuire, W. L. Association of p53 protein expression with tumor cell proliferation rate and clinical outcome in node-negative breast cancer. J. Natl. Cancer Inst. (Bethesda), *85:* 200–206, 1993.
5. Teixeira, C., Reed, J. C., and Pratt, M. A. Estrogen promotes chemotherapeutic drug resistance by a mechanism involving *Bcl-2* proto-oncogene expression in human breast cancer cells. Cancer Res., *55:* 3902–3907, 1995.
6. Haldar, S., Basu, A., and Croce, C. M. Bcl-2 is the guardian of microtubule integrity. Cancer Res., *57:* 229–233, 1997.
7. Leek, R. D., Kaklamanis, L., Pezzella, F., Gatter, K. C., and Harris, A. L. bcl-2 in normal human breast and carcinoma, association with oestrogen receptor-positive, epidermal growth factor receptor-negative tumours and *in situ* cancer. Br. J. Cancer, *69:* 135–139, 1994.

[5] National Cancer Institute Clinical Cancer Trials. Internet address: http://cancertrials.nci.nih.gov200.

8. Nunez, G., London, L., Hockenbery, D., Alexander, M., Mckearn, J. P., and Korsmeyer, S. J. Deregulated *Bcl-2* gene expression selectively prolongs survival of growth factor-deprived hemopoietic cell lines. J. Immunol., *144:* 3602–3610, 1990.
9. McDonnell, T. J., Troncoso, P., Brisbay, S. M., Logothetis, C., Chung, L. W. K., Hsieh, J., Tu, S., and Campbell, M. L. Expression of the protooncogene *bc1-2* in prostate and its association with emergence of androgen- independent prostate cancer. Cancer Res., *52:* 6940–6944, 1992.
10. Sato, N., Saga, T., Sakahara, H., Yao, Z., Nakamoto, Y., Zhang, M., Kuroki, M., Matsuoka, Y., Iida, Y., and Konishi, J. Intratumoral distribution of radiolabeled antibody and radioimmunotherapy in experimental liver metastases model of nude mouse. J. Nucl. Med., *40:* 685–692, 1999.
11. DeNardo, S. J., Kukis, D. L., Miers, L. A., Winthrop, M. D., Kroger, L. A., Salako, Q., Shen, S., Lamborn, K. R., Gumerlock, P. H., Meares, C. F., and DeNardo, G. L. Yttrium-90-DOTA-peptide-chimeric L6 radioimmunoconjugate: Efficacy and toxicity in mice bearing p53 mutant human breast cancer xenografts. J. Nucl. Med., *39:* 842–849, 1998.
12. Buchsbaum, D. J. Experimental radioimmunotherapy. Semin. Radiat. Oncol., *10:* 156–167, 2000.
13. Jain, R. K., and Baxter, L. T. Mechanisms of heterogeneous distribution of monoclonal antibodies and other macromolecules in tumors: significance of elevated interstitial pressure. Cancer Res., *48:* 7022–7032, 1988.
14. Burke, P. A., and DeNardo, S. J. Antiangiogenic agents and their promising potential for combined therapy. Crit. Rev. Oncol./Hematol., *39:* 155–171, 2001.
15. Denekamp, J. Vascular endothelium as the vulnerable element in tumours. Acta Radiol. Oncol., *23:* 217–225, 1984.
16. Cheresh, D. A. Integrins: structure, function and biological properties. Adv. Mol. Cell Biol., *6:* 225–252, 1993.
17. Max, R., Gerritsen, R. R., Nooijen, P. T., Goodman, S. L., Sutter, A., Keilholz, U., Ruiter, D. J., and De Waal, R. M. Immunohistochemical analysis of integrin $\alpha_v\beta_3$ expression on tumor-associated vessels of human carcinomas. Int. J. Cancer, *71:* 320–324, 1997.
18. Brooks, P. C., Stromblad, S., Klemke, R., Visscher, D., Sarkar, F. H., and Cheresh, D. A. Antiintegrin $\alpha_v\beta_3$ blocks human breast cancer growth and angiogenesis in human skin. J. Clin. Investig., *96:* 1815–1822, 1995.
19. Brooks, P. C., Montgomery, A. M., Rosenfeld, M., Reisfeld, R. A., Hu, T., Klier, G., and Cheresh, D. A. Integrin $\alpha_v\beta_3$ antagonists promote tumor regression by inducing apoptosis of angiogenic blood vessels. Cell, *79:* 1157–1164, 1994.
20. Brooks, P. C., Clark, R. A., and Cheresh, D. A. Requirement of vascular integrin $\alpha_v\beta_3$ for angiogenesis. Science (Wash. DC), *264:* 569–571, 1994.
21. Varner, J. A. The role of vascular cell integrins v3 and v5 in angiogenesis. EXS (Basel), *97:* 361–390, 1997.
22. Gasparini, G., Brooks, P. C., Biganzoli, E., Vermeulen, P. B., Bonoldi, E., Dirix, L. Y., Ranieri, G., Miceli, R., and Cheresh, D. A. Vascular integrin $\alpha_v\beta_3$: a new prognostic indicator in breast cancer. Clin. Cancer Res., *4:* 2625–2634, 1998.
23. Felding-Habermann, B., O'Toole, T. E., Smith, J. W., Fransvea, E., Ruggeri, Z. M., Ginsberg, M. H., Hughes, P. E., Pampori, N., Shattil, S. J., Saven, A., and Mueller, B. M. Integrin activation controls metastasis in human breast cancer. Proc. Natl. Acad. Sci. USA, *98:* 1853–1858, 2001.
24. Qiao, R., Yan, W., Lum, H., and Malik, A. B. Arg-Gly-Asp peptide increases endothelial hydraulic conductivity: comparison with thrombin response. Am. J. Physiol., *269:* C110–C117, 1995.
25. Mitjans, F., Meyer, T., Fittschen, C., Goodman, S. L., Jonczyk, A., Marshall, J. F., Reyes, G., and Piulats, J. *In vivo* therapy of malignant melanoma by means of antagonists of v integrins. Int. J. Cancer, *87:* 716–723, 2000.
26. Allman, R., Cowburn, P., and Mason, M. *In vitro* and *in vivo* effects of a cyclic peptide with affinity for the $\alpha_v\beta_3$ integrin in human melanoma cells. Eur. J. Cancer, *36:* 410–422, 2000.
27. Lode, H. N., Moehler, T., Xiang, R., Jonczyk, A., Gillies, S. D., Cheresh, D. A., and Reisfeld, R. A. Synergy between an anti-angiogenic intergrin $_v$ antagonist and an antibody-cytokine fusion protein eradicates spontaneous tumor metastases. Proc. Natl. Acad. Sci. USA, *96:* 1591–1596, 1999.
28. Haubner, R., Wester, H. J., Reuning, U., Senekowitsch-Schmidtke, R., Diefenbach, B., Kessler, H., Stocklin, G., and Schwaiger, M. Radiolabeled $\alpha_v\beta_3$ integrin antagonists: a new class of tracers for tumor targeting. J. Nucl. Med., *40:* 1061–1071, 1999.
29. Haubner, R., Wester, H. J., Burkhart, F., Senekowitsch-Schmidtke, R., Weber, W., Goodman, S. L., Kessler, H., and Schwaiger, M. Glycosylated RGD-containing peptides: tracer for tumor targeting and angiogenesis imaging with improved biokinetics. J. Nucl. Med., *42:* 326–336, 2001.
30. DeNardo, S. J., Burke, P. A., Leigh, B. R., O'Donnell, R. T., Miers, L. A., Kroger, L. A., Goodman, S. L., Matzku, S., Jonczyk, A., Lamborn, K. R., and DeNardo, G. L. Neovascular targeting with cyclic RGD peptide (cRGDf-ACHA) to enhance delivery of radioimmunotherapy. Cancer Biother. Radiopharm., *15:* 71–79, 2000.
31. Dechantsreiter, M. A., Plankar, E., Matha, B., Lohof, E., Holzemann, G., Jonczyk, A., Goodman, S. L., and Kessler, H. *N*-Methylated cyclic RGD peptides as highly active and selective avb3 integrin antagonists. J. Med. Chem., *42:* 3033–3040, 1999.
32. Fell, H. P., Gayle, M. A., Yelton, D., Lipsich, L., Schieven, G. L., Marken, J. S., Aruffo, A., Hellstrom, K. E., Hellstrom, I., and Bajorath, J. Chimeric L6 anti-tumor antibody. Genomic construction, expression, and characterization of the antigen binding site. J. Biol. Chem., *267:* 15552–15558, 1992.
33. Liu, A. Y., Robinson, R. R., Hellstrom, K. E., Murray, E. D. J., Chang, C. P., and Hellstrom, I. Chimeric mouse-human IgG1 antibody that can mediate lysis of cancer cells. Proc. Natl. Acad. Sci. USA, *84:* 3439–3443, 1987.
34. Hellstrom, I., Horn, D., Linsley, P., Brown, J. P., Brankovan, V., and Hellstrom, K. E. Monoclonal antibodies raised against human lung carcinomas. Cancer Res., *46:* 3917–3923, 1986.
35. Marken, J. S., Bajorath, J., Edwards, C. P., Farr, A. G., Schieven, G. L., Hellstrom, I., Hellstrom, K. E., and Aruffo, A. Membrane topology of the L6 antigen and identification of the protein epitope recognized by the L6 monoclonal antibody. J. Biol. Chem., *269:* 7397–7401, 1994.
36. Howell, L. P., DeNardo, S. J., Levy, N., Lund, J., and DeNardo, G. L. Immunohistochemical staining of metastatic ductal carcinomas of the breast by monoclonal antibodies used in imaging and therapy: a comparative study. Int. J. Biol. Markers, *10:* 126–135, 1995.
37. Winthrop, M. D., DeNardo, S. J., Muenzer, J. T., Chi, S. G., and Gumerlock, P. H. p53-independent response of a human breast cancer xenograft to radioimmunotherapy. Cancer (Phila.), *80* (Suppl.)*:* 2529–2537, 1997.
38. DeNardo, S. J., Zhong, G.-R., Salako, Q., Li, M., DeNardo, G. L., and Meares, C. F. Pharmacokinetics of chimeric L6 conjugated to indium-111 and yttrium-90-DOTA-peptide in tumor bearing mice. J. Nucl. Med., *36:* 829–836, 1995.
39. Li, M., Meares, C. F., Salako, Q., Kukis, D. L., Zhong, G.-R., Miers, L. A., and DeNardo, S. J. Prelabeling of chimeric monoclonal antibody L6 with ^{90}Yttrium- and ^{111}Indium-1,4,7,10-tetraazacyclododecane-*N*,*N*′,*N*″,*N*‴-tetraacetic acid (DOTA) chelates for radioimmunodiagnosis and therapy. Cancer Res. *55* (Suppl.)*:* 5726–5728, 1995.
40. Burke, P. A., DeNardo, S. J., Miers, L. A., Kukis, D. L., and DeNardo, G. L. Combined modality radioimmunotherapy: promise and peril. Clin. Cancer Res., *94:* 1320–1331, 2002.
41. DeNardo, G. L., Kukis, D. L., Shen, S., Mausner, L. F., Meares, C. F., Srivastava, S. C., Miers, L. A., and DeNardo, S. J. Efficacy and toxicity of ^{67}Cu-2IT-BAT-Lym-1 radioimmunoconjugate in mice implanted with Burkitt's lymphoma (Raji). Clin. Cancer Res., *3:* 71–79, 1997.
42. Seiverd, C. E. Hematology for Medical Technologists, pp. 91–432. Philadelphia: Lea and Febiger, 1972.
43. Gavrieli, Y., Sherman, Y., and Ben-Sasson, S. A. Identification of programmed cell death *in-situ* via specific labeling of nuclear DNA fragmentation. J. Cell Biol., *119:* 493–501, 1992.
44. Stadelmann, C., and Lassmann, H. Detection of apoptosis in tissue sections. Cell Tissue Res., *301:* 19–31, 2000.
45. Kerr, J. F. R., Winterford, C. M., and Harmon, B. V. Apoptosis. Its significance in cancer and cancer therapy. Cancer (Phila.), *73:* 2013–2026, 1994.
46. Weidner, N., Folkman, J., Pozza, F., Pierantonio, B., Allred, E. N., Moore, D. H., Meli, S., and Gasparini, G. Tumor angiogenesis: a new significant and independent prognostic indicator in early-stage breast carcinoma. J. Natl. Cancer Inst. (Bethesda), *84:* 1875–1887, 1992.
47. Shalinsky, D. R., Brekken, J., Zou, H., Bloom, L. A., McDermott, C. D., Zook, S., Varki, N. M., and Appelt, K. Marked antiangiogenic and antitumor efficacy of AG3340 in chemoresistant human non-small cell lung cancer tumors: single agent and combination chemotherapy studies. Clin. Cancer Res., *5:* 1905–1917, 1999.
48. Gerdes, J., Lemke, H., Baisch, H., Wacher, H., Schwab, U., and Stein, H. Cell cycle analysis of a cell proliferation-associated human nuclear antigen defined by the monoclonal antibody Ki-67. J. Immunol., *133:* 1710–1715, 1984.
49. Gerdes, J., Li, L., Schluter, C., Duchrow, M., Wohlenber, C., Gerlach, C., Stahmaer, I., Kloth, S., Brandt, E., and Flad, H. Immunobiochemical and molecular biologic characterization of the cell proliferation-associated nuclear antigen that is defined by monoclonal antibody Ki-67. Am. J. Pathol., *138:* 867–873, 1991.
50. Kinuya, S., Kawashima, A., Yokoyama, K., Kudo, M., Kasahara, Y., Watanabe, N., Shuke, N., Bunko, H., Michigishi, T., and Tonami, N. Anti-angiogenic therapy and radioimmunotherapy in colon cancer xenografts. Eur. J. Nucl. Med., *28:* 1306–1312, 2001.
51. Stein, R., Chen, S., Reed, L., Richel, H., and Goldenberg, D. M. Combining radioimmunotherapy and chemotherapy for treatment of medullary thyroid carcinoma. Cancer (Phila.), *94:* 51–61, 2002.
52. Cardillo, T. M., Blumenthal, R. D., Ying, Z., and Gold, D. V. Combined gemcitabine and radioimmunotherapy for the treatment of pancreatic cancer. Int. J. Cancer, *97:* 386–392, 2002.
53. Pedley, R. B., Hill, S. A., Boxer, G. M., Flynn, A. A., Boden, R., Watson, R., Dearling, J., Chaplin, D. J., and Begent, R. H. J. Eradication of colorectal xenografts by combined radioimmunotherapy and combretastatin A-4 3-*O*-Phosphate. Cancer Res., *61:* 4716–4722, 2001.
54. Ng, B., Kramer, E., Liebes, L., Wasserheit, C., Hochster, H., Blank, E., Ceriani, R., and Furmanski, P. Radiosensitization of tumor-targeted radioimmunotherapy with prolonged topotecan infusion in human breast cancer xenografts. Cancer Res., *61:* 2996–3001, 2001.
55. Blumenthal, R. D., Taylor, A., Osorio, L., Ochakovskaya, R., Raleigh, J. A., Papadopoulou, M., Bloomer, W. D., and Goldenberg, D. M. Optimizing the use of combined radioimmunotherapy and hypoxic cytotoxin therapy as a function of tumor hypoxia. Int. J. Cancer, *94:* 564–571, 2001.
56. van Gog, F. B., Brakenhoff, R. H., Stigter-van Walsum, M., Snow, G. B., and van Dongen, G. A. Perspectives of combined radioimmunotherapy and anti-EGFR antibody therapy for the treatment of residual head and neck cancer. Int. J. Cancer, *77:* 13–18, 1998.
57. DeNardo, S. J., Kroger, L. A., Lamborn, K. R., Miers, L. A., Kukis, D. L., O'Donnell, R., Richman, C., and DeNardo, G. L. Importance of temporal relationships in combined modality radioimmunotherapy of breast carcinoma. Cancer (Phila.), *80* (Suppl.)*:* 2583–2590, 1997.
58. Clarke, K., Lee, F. T., Brechbiel, M. W., Smyth, F. E., Old, L. J., and Scott, A. M. Therapeutic efficacy of anti-Lewis(y) humanized 3S193 radioimmunotherapy in a breast cancer model: enhanced activity when combined with Taxol chemotherapy. Clin. Cancer Res., *6:* 3621–3628, 2000.
59. O'Donnell, R. T., DeNardo, S. J., Miers, L., Lamborn, K. R., Kukis, D. L., DeNardo, G. L., and Meyers, F. J. Combined modality radioimmunotherapy for human prostate

cancer xenografts with taxanes and ^{90}Yttrium-DOTA-peptide-ChL6. Prostate, *50:* 27–37, 2002.
60. O'Donnell, R., DeNardo, S. J., Miers, L. A., Kukis, D. L., Mirick, G. R., Kroger, L. A., and DeNardo, G. L. Combined modality radioimmunotherapy with Taxol and ^{90}Y-Lym-1 for Raji lymphoma xenografts. Cancer Biother. Radiopharm., *13:* 351–361, 1998.
61. Kennel, S. J., Lankford, T. K., Foote, L. J., Davis, I. A., Boll, R. A., and Mirzadeh, S. Combination vascular targeted and tumor targeted radioimmunotherapy. Cancer Biother. Radiopharm., *14:* 371–379, 1999.
62. Mauceri, H. J., Hanna, N. N., Beckett, M. A., Gorski, D. H., Staba, M. J., Stellato, K. A., Bigelow, K., Heimann, R., Gately, S., Dhanabal, M., Soff, G. A., Sukhatme, V. P., Kufe, D. W., and Weichselbaum, R. Combined effects of angiostatin and ionizing radiation in autitumour therapy. Nature (Lond.), *394:* 287–291, 1998.
63. Gorski, D. H., Mauceri, H. J., Salloum, R. M., Gately, S., Hellman, S., Beckett, M. A., Sukhatme, V. P., Soff, G. A., Kufe, D. W., and Weichselbaum, R. R. Potentiation of the antitumor effect of ionizing radiation by brief concomitant exposures to angiostatin. Cancer Res., *58:* 5686–5689, 1998.
64. Hanna, N. N., Seetharam, S., Mauceri, H. J., Beckett, M. A., Jaskowiak, N. T., Salloum, R. M., Hari, D., Dhanabal, M., Ramchandran, R., Kalluri, R., Sukhatme, V. P., Kufe, D. W., and Weichselbaum, R. R. Antitumor interaction of short-course endostatin and ionizing radiation. Cancer J., *6:* 287–293, 2000.
65. Teicher, B. A. Potentiation of cytotoxic cancer therapies by antiangiogenic agents. *In:* B. A. Teicher (ed.), Antiangiogenic Agents in Cancer Therapy, pp. 277–316. Totowa, NJ: Humana Press. 1999.
66. Lund, E. L., Bastholm, L., and Kristjansen, P. E. G. Therapeutic synergy of TNP-470 and ionizing radiation: effects on tumor growth, vessel morphology, and angiogenesis in human glioblastoma multiforme xenografts. Clin. Cancer Res., *6:* 971–978, 2000.
67. Gorski, D. H., Beckett, M. A., Jaskowiak, N. T., Calvin, D. P., Mauceri, H. J., Salloum, R. M., Seetharam, S., Koons, A., Hari, D. M., Kufe, D. W., and Weichselbaum, R. R. Blockade of the vascular endothelial growth factor stress response increases the antitumor effects of ionizing radiation. Cancer Res., *59:* 3374–3378, 1999.
68. Lee, C., Heijn, M., Tomaso, E., Griffon-Etienne, G., Ancukiewicz, M., Koike, C., Park, K. R., Ferrara, N., Jain, R. K., Suit, H. D., and Boucher, Y. Anti-vascular endothelial growth factor treatment augments tumor radiation response under normoxic or hypoxic conditions. Cancer Res., *60:* 5565–5570, 2000.
69. Kozin, S. V., Boucher, Y., Hicklin, D. J., Bohlen, P., Jain, R. K., and Suit, H. D. Vascular endothelial growth factor receptor-2-blocking antibody potentiates radiation-induced long-term control of human tumor xenografts. Cancer Res., *61:* 39–44, 2001.
70. Geng, L., Donnelly, E., McMahon, G., Lin, P. C., Sierra-Rivera, E., Oshinka, H., and Hallahan, D. E. Inhibition of vascular endothelial growth factor receptor signaling leads to reversal of tumor resistance to radiotherapy. Cancer Res., *61:* 2413–2419, 2001.
71. Hess, C., Vuong, V., Hegyi, I., Riesterer, O., Wood, J., Fabbro, D., Glanzmann, C., Bodis, S., and Pruschy, M. Effect of VEGF receptor inhibitor PTK787/ZK222548 combined with ionizing radiation on endothelial cells and tumour growth. Br. J. Cancer, *85:* 2010–2016, 2001.
72. Salloum, R. M., Jaskowiak, N. T., Mauceri, H. J., Seetharam, S., Beckett, M. A., Koons, A. M., Hari, D. M., Gupta, V. K., Reimer, C., Kalluri, R., Posner, M. C., Hellman, S., Kufe, D. W., and Weichselbaum, R. R. NM-3, an isocoumarin, increases the antitumor effects of radiotherapy without toxicity. Cancer Res., *60:* 6958–6963, 2000.
73. Stromblad, S., Becker, J. C., Yebra, M., Brooks, P. C., and Cheresh, D. A. Suppression of p53 activity and p21$^{WAF1/CIP1}$ expression by vascular cell integrin $\alpha_V\beta_3$ during angiogenesis. J. Clin. Investig., *98:* 426–433, 1996.
74. Mitjans, F., Sander, D., Adan, J., Sutter, A., Martinez, J. M., Jaggle, C.-S., Moyano, J. M., Kreysch, H.-G., Piulats, J., and Goodman, S. L. An anti-a_V-integrin antibody that blocks integrin function inhibits the development of a human melanoma in nude mice. J. Cell Sci., *108:* 2825–2838, 1995.
75. MacDonald, T. J., Taga, T., Shimada, H., Tabrizi, P., Zlokovic, B. V., and Cheresh, D. A. Preferential susceptibility of brain tumors to the antiangiogenic effects of v integrin antagonist. Neurosurgery, *48:* 151–157, 2001.
76. Sorbera, L. A., Graul, A., and Castaner, J. Cilengitide. Oncolytic, angiogenesis inhibitor, integrin $\alpha_V\beta_3$, $\alpha_V\beta_5$ antagonist: EMD-121974, EMD-85189. Drugs Future, *25:* 674–678, 2000.
77. Browder, T., Butterfield, C. E., Kraling, B. M., Shi, B., Marshall, B., O'Reilly, M. S., and Folkman, J. Antiangiogenic scheduling of chemotherapy improves efficacy against experimental drug-resistant cancer. Cancer Res., *60:* 1878–1886, 2000.
78. Bruns, C. J., Liu, W., Davis, D. W., Shaheen, R. M., McConkey, D. J., Wilson, M. R., Bucana, C. D., Hicklin, D. J., and Ellis, L. M. Vascular endothelial growth factor is an *in vivo* survival factor for tumor endothelium in a murine model of colorectal carcinoma liver metastases. Cancer (Phila.), *89:* 488–499, 2000.
79. Hallahan, D. E., Staba-Hogan, M. J., Virudachalam, S., and Kolchinsky, A. X-ray-induced P-selectin localization to the lumen of tumor vessels. Cancer Res., *58:* 5216–5220, 1998.
80. Hallahan, D. E., Geng, L., Cmelak, A. J., Chakravarthy, A. B., Martin, W., Scarfone, C., and Gonzalez, A. Targeting drug delivery to radiation-induced neoantigens in tumor microvasculature. J. Controlled Release, *74:* 183–191, 2001.
81. Bombeli, T., Schwartz, B. R., and Harlan, J. M. Adhesion of activated platelets to endothelial cells: evidence for a GPIIbIIIa-dependent bridging mechanism and novel roles for endothelial intercellular adhesion molecule 1 (ICAM-1), $\alpha_v\beta_3$ integrin, and GPIBα. J. Exp. Med., *187:* 329–339, 1998.
82. Browder, T., Folkman, J., and Pirie-Shepherd, S. The hemostatic system as a regulator of angiogenesis. J. Biol. Chem., *275:* 1521–1524, 2000.
83. Verheul, H. M., Hoekman, K., Lupu, F., Broxterman, H. J., van der Valk, P., Kakkar, A. K., and Pinedo, H. M. Platelet and coagulation activation with vascular endothelial growth factor generation in soft tissue sarcomas. Clin. Cancer Res., *6:* 166–171, 2000.
84. Soldi, R., Mitola, S., Strasly, M., Defilippi, P., Tarone, G., and Bussolino, F. Role of $\alpha_v\beta_3$ integrin in the activation of vascular endothelial growth factor receptor-2. EMBO J., *18:* 882–892, 1999.
85. Moehler, T. M., Neben, K., Ho, A. D., and Goldschmidt, H. Angiogenesis in hematologic malignancies. Ann. Hematol., *80:* 695–705, 2001.
86. DeNardo, S. J., Gumerlock, P. H., Winthrop, M. D., Mack, P. C., Chi, S. G., Lamborn, K. R., Shen, S., Miers, L. A., deVere White, R. W., and DeNardo, G. L. Yttrium-90 chimeric L6 therapy of human breast cancer in nude mice and apoptosis-related messenger RNA expression. Cancer Res., *55* (Suppl.)*:* 5837–5841, 1995.

Cancer Research
The Journal of Cancer Research (1916–1930) | The American Journal of Cancer (1931–1940)

AACR American Association for Cancer Research

Cilengitide Targeting of $\alpha_v\beta_3$ Integrin Receptor Synergizes with Radioimmunotherapy to Increase Efficacy and Apoptosis in Breast Cancer Xenografts

Patricia A. Burke, Sally J. DeNardo, Laird A. Miers, et al.

Cancer Res 2002;62:4263-4272.